Retrieval and Variability of Stratospheric Aerosols from SCIAMACHY Limb-scatter Observations

L. A. Brinkhoff[1],
A. Rozanov[1], F. Ernst[1], C. von Savigny[2],
R. Hommel[1], H. Bovensmann[1], and J. P. Burrows[1]

1. Institute of Environmental Physics and Remote Sensing, University of Bremen, Bremen, Germany
2. Institute of Physics, Ernst-Moritz-Arndt-University of Greifswald, Greifswald, Germany

SCIAMACHY/Envisat limb measurements

Operating time: March 2002 – April 2012
Orbit information: sun-synchronous, ~800 km altitude

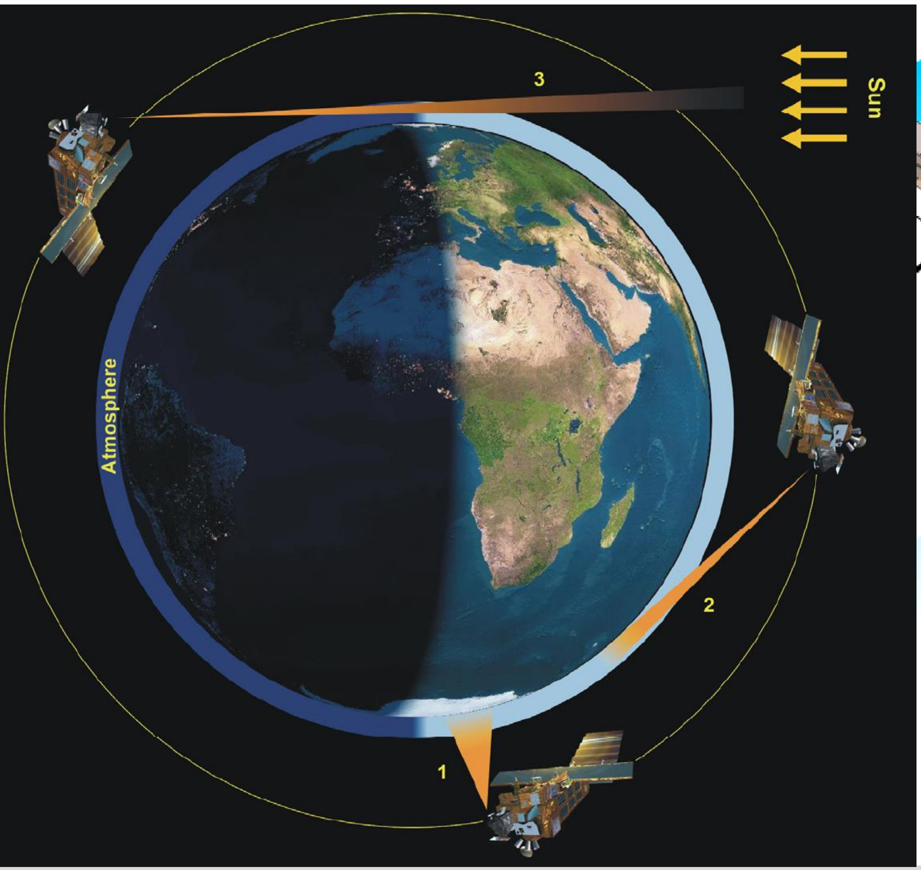

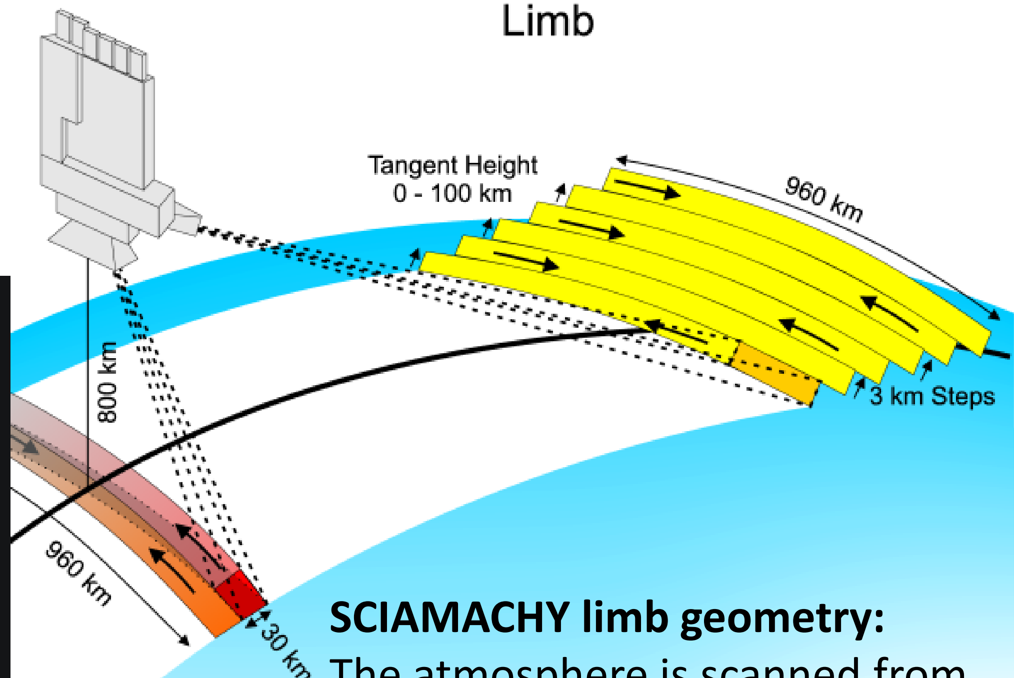

SCIAMACHY limb geometry:
The atmosphere is scanned from 0 km to ~93 km with tangent height steps of 3.3 km, measuring scattered solar radiation.

Spatial resolution:
[4 × 240 × 400] km
(vert. × across × along flight dir.)

Universität Bremen*

This presentation participates in the student award contest

Retrieval method

Generating the measurement vector (Bourassa et al., 2007)

1. $$I_N^{\lambda}(TH) = I^{\lambda}(TH)/I^{\lambda}(TH_{ref})$$

with $TH_{ref} = 35\,\mathrm{km}$

2. $$y(TH) = \ln\left(\frac{I_N^{\lambda_l}(TH)}{I_N^{\lambda_s}(TH)}\right)$$

with $\lambda_s = 470\,\mathrm{nm}$ and $\lambda_l = 750\,\mathrm{nm}$

Inverse problem

$$\tilde{\mathbf{y}} = \mathbf{K}\hat{x} + \epsilon$$

State vector: $\hat{x} = (x - x_0)/x_0$

Measurement vector: $\tilde{\mathbf{y}} = y - y_0$

K: Weighting function matrix

ϵ: Error

x_0: A priori profile

y_0: Simulated radiance profile

'Optimal Estimation' method (Rodgers, 2000)

$$\|\mathbf{K}\hat{x} - \tilde{\mathbf{y}}\|^2_{S_{\mathbf{y}}^{-1}} + \|\hat{x}\|^2_{S_a^{-1}}$$ is minimized.

S_y: Error covariance matrix of y

S_a: Error covariance matrix of x_0

Retrieval method

For more information, see
Florian Ernst (poster board 2)

Generating the meas

1. $\boldsymbol{I}_N^{\lambda}(TH) = \boldsymbol{I}^{\lambda}(TH)/\boldsymbol{I}^{\lambda}(TH_{ref})$

with $TH_{ref} = 35\,\mathrm{km}$

2. $\boldsymbol{y}(TH) = \ln\left(\frac{\boldsymbol{I}_N^{\lambda_l}(TH)}{\boldsymbol{I}_N^{\lambda_s}(TH)}\right)$

with $\lambda_s = 470\,\mathrm{nm}$ and $\lambda_l = 750\,\mathrm{nm}$

Inverse problem

$$\tilde{\mathbf{y}} = \mathbf{K}\hat{\boldsymbol{x}} + \epsilon$$

State vector: $\hat{\boldsymbol{x}} = (\boldsymbol{x} - \boldsymbol{x}_0)/\boldsymbol{x}_0$

Measurement vector: $\tilde{\mathbf{y}} = \boldsymbol{y} - \boldsymbol{y}_0$

K: Weighting function matrix
ϵ: Error

x_0: A priori profile
y_0: Simulated radiance profile from x_0

'Optimal Estimation' method (Rodgers, 2000)

$$\|\mathbf{K}\hat{\boldsymbol{x}} - \tilde{\mathbf{y}}\|^2_{S_{\mathbf{y}}^{-1}} + \|\hat{\boldsymbol{x}}\|^2_{S_a^{-1}}$$ is minimized.

S_y: Error covariance matrix of y
S_a: Error covariance matrix of x_0

Outline

1. Climatological interpretation of the SCIAMACHY stratospheric aerosol data set (V1.1)

2. Outlook
   I) trend analysis
   II) the estimation of the stratospheric aerosol particle size distribution

Volcano and bushfire observations

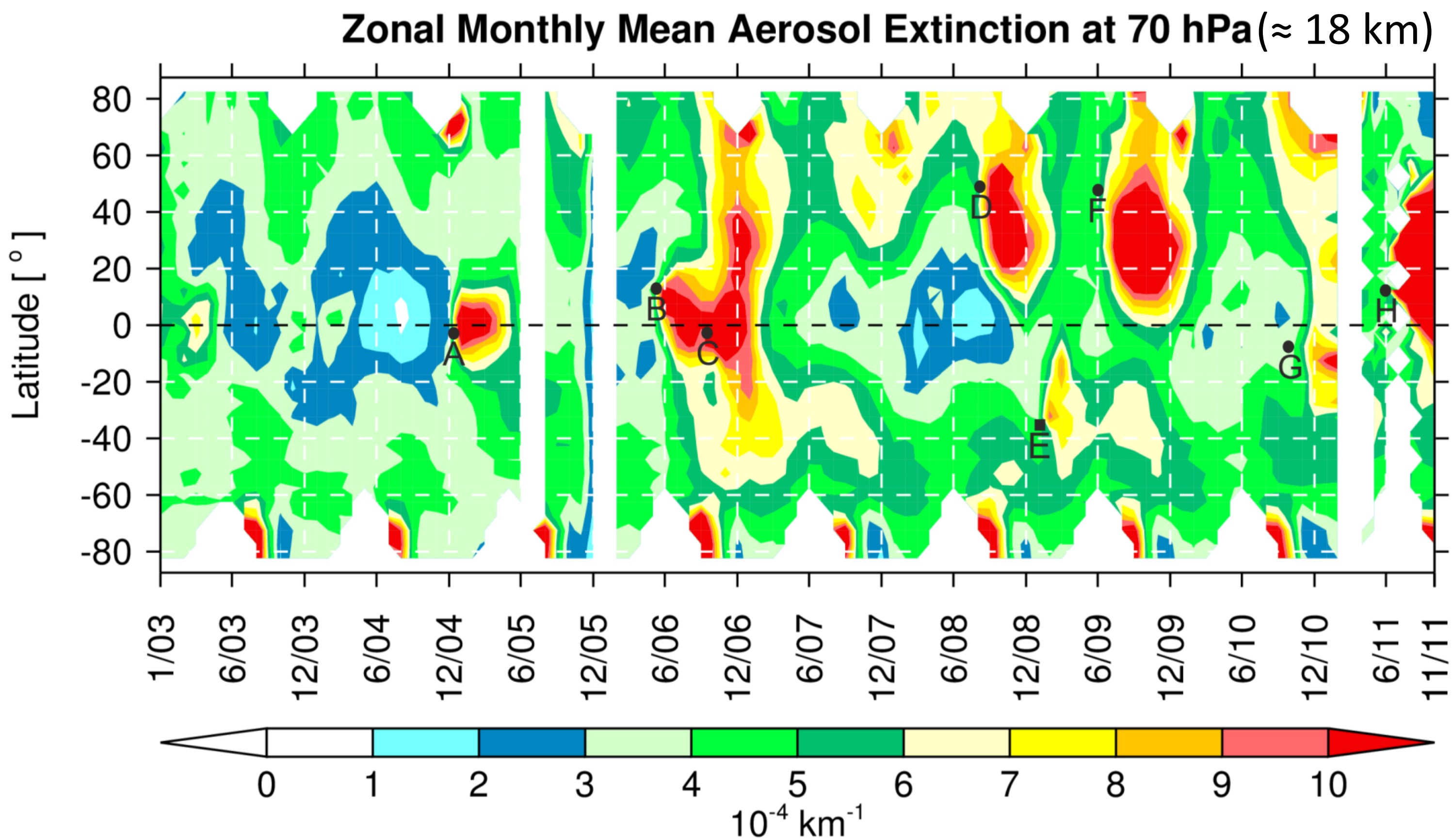

A) Manam, Jan `05, 4°S
B) Soufriere Hills, May `06, 16°N
C) Tavurvur, Oct `06, 4°S
D) Kasatochi, Aug `08, 52°N
E) Black Saturday Australia, 7 Feb-14 March `09 37°S
F) Sarychev Peak, June `09, 48°N
G) Mount Merapi, Oct `10, 7°S
H) Nabro, June `11, 13°N

Volcano and bushfire observations

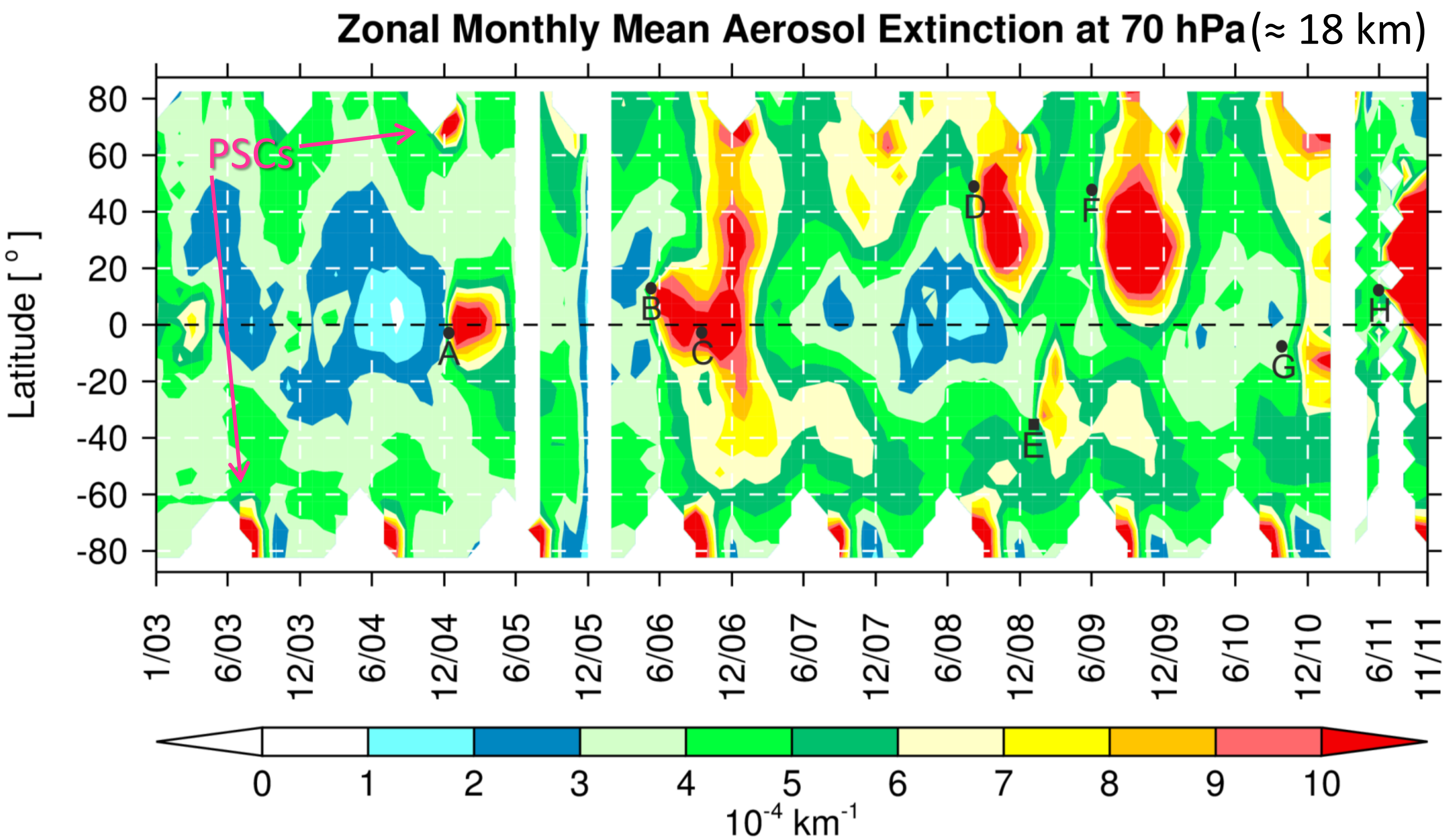

A) Manam, Jan `05, 4°S
B) Soufriere Hills, May `06, 16°N
C) Tavurvur, Oct `06, 4°S
D) Kasatochi, Aug `08, 52°N
E) Black Saturday Australia, 7 Feb-14 March `09 37°S
F) Sarychev Peak, June `09, 48°N
G) Mount Merapi, Oct `10, 7°S
H) Nabro, June `11, 13°N

Comparison of the pattern with CALIPSO

SCIAMACHY zonal monthly mean aerosol extinction at 525 nm and 70 hPa ≈ 18 km.

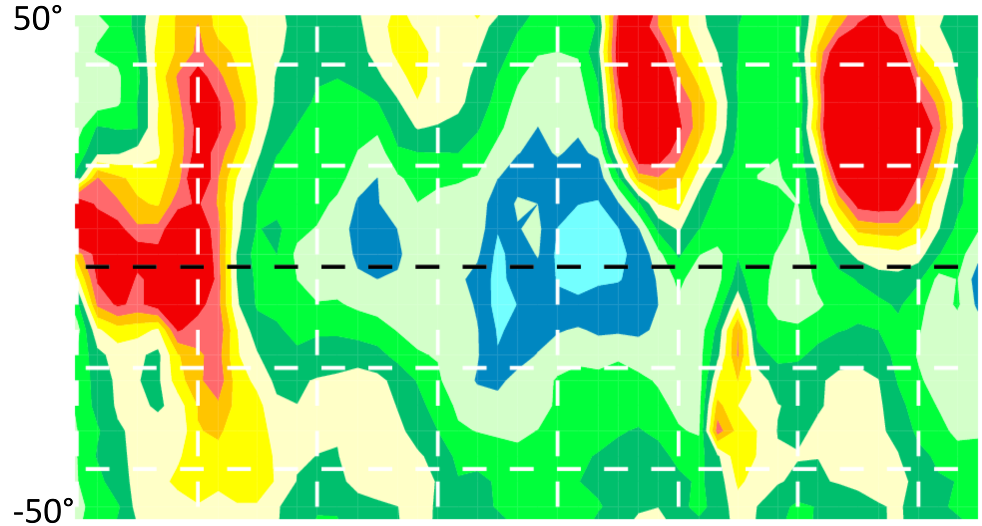

Zonal mean scattering ratio at 532 nm, 17-21 km from **CALIPSO** lidar measurements, June '06–March '10. From Solomon et al. (2011)

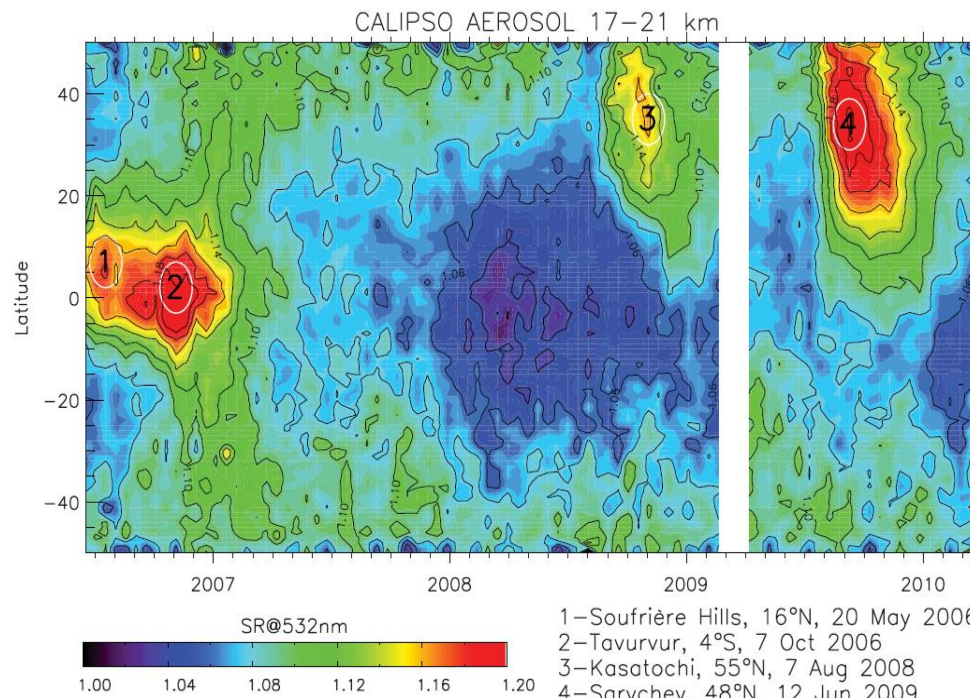

Latitude-time cross section at **20 hPa** (≈ 26 km)

Seasonal cycle

with maximum aerosol load in winter.

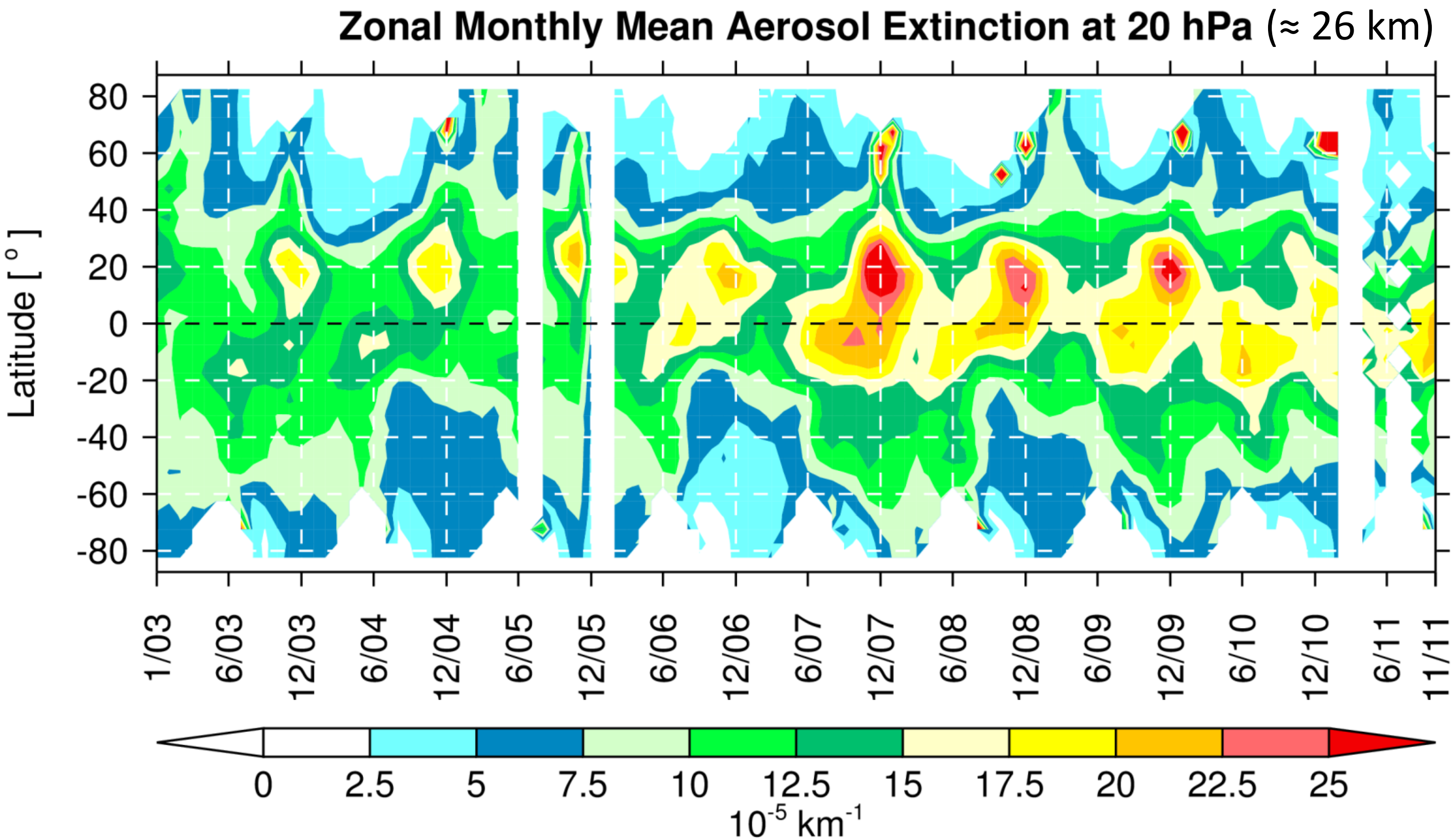

Seasonal cycle

… can be explained by the Brewer-Dobson circulation

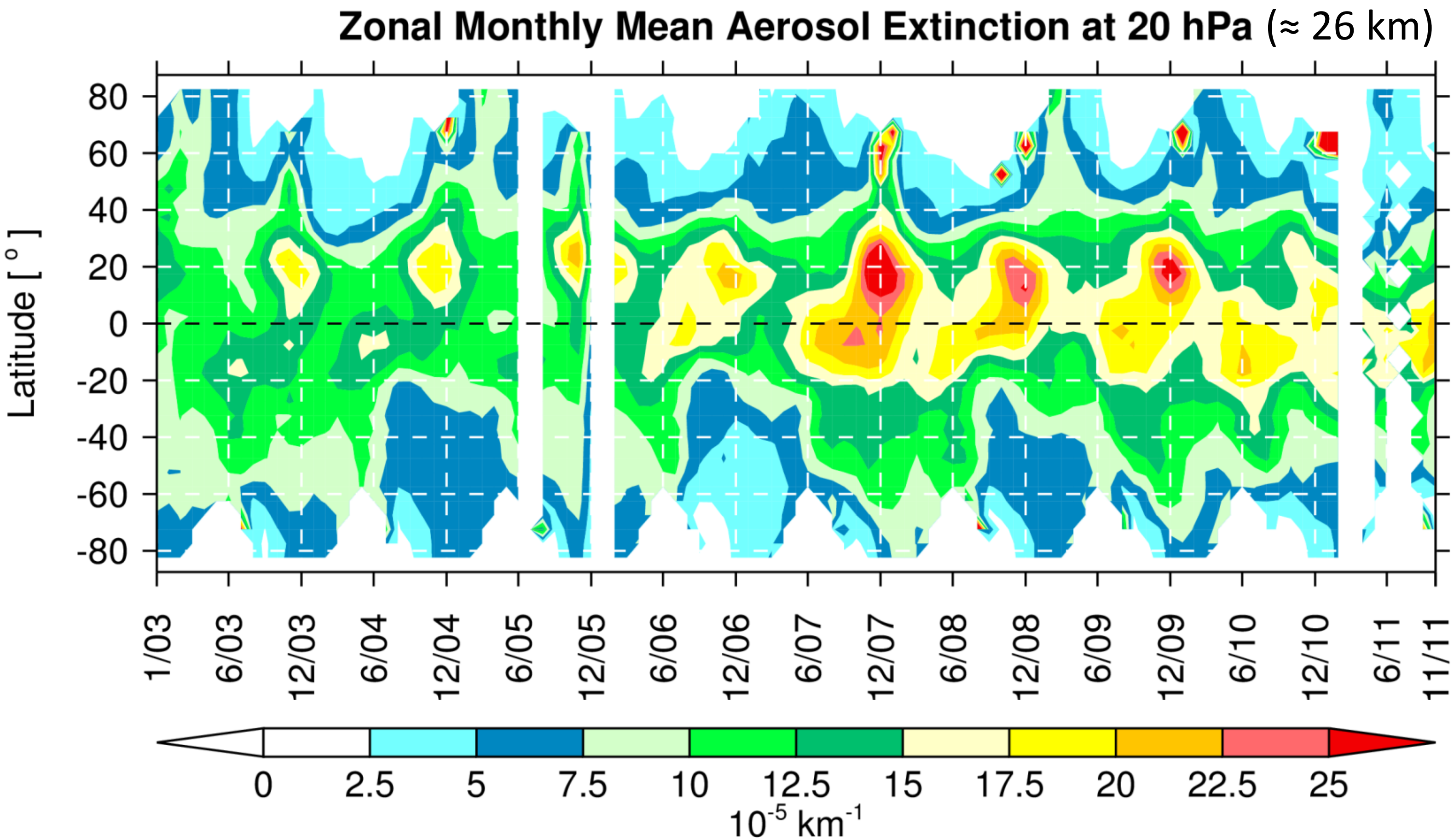

Seasonal cycle

… can be explained by the Brewer-Dobson circulation, which is

1. stronger in the winter hemisphere

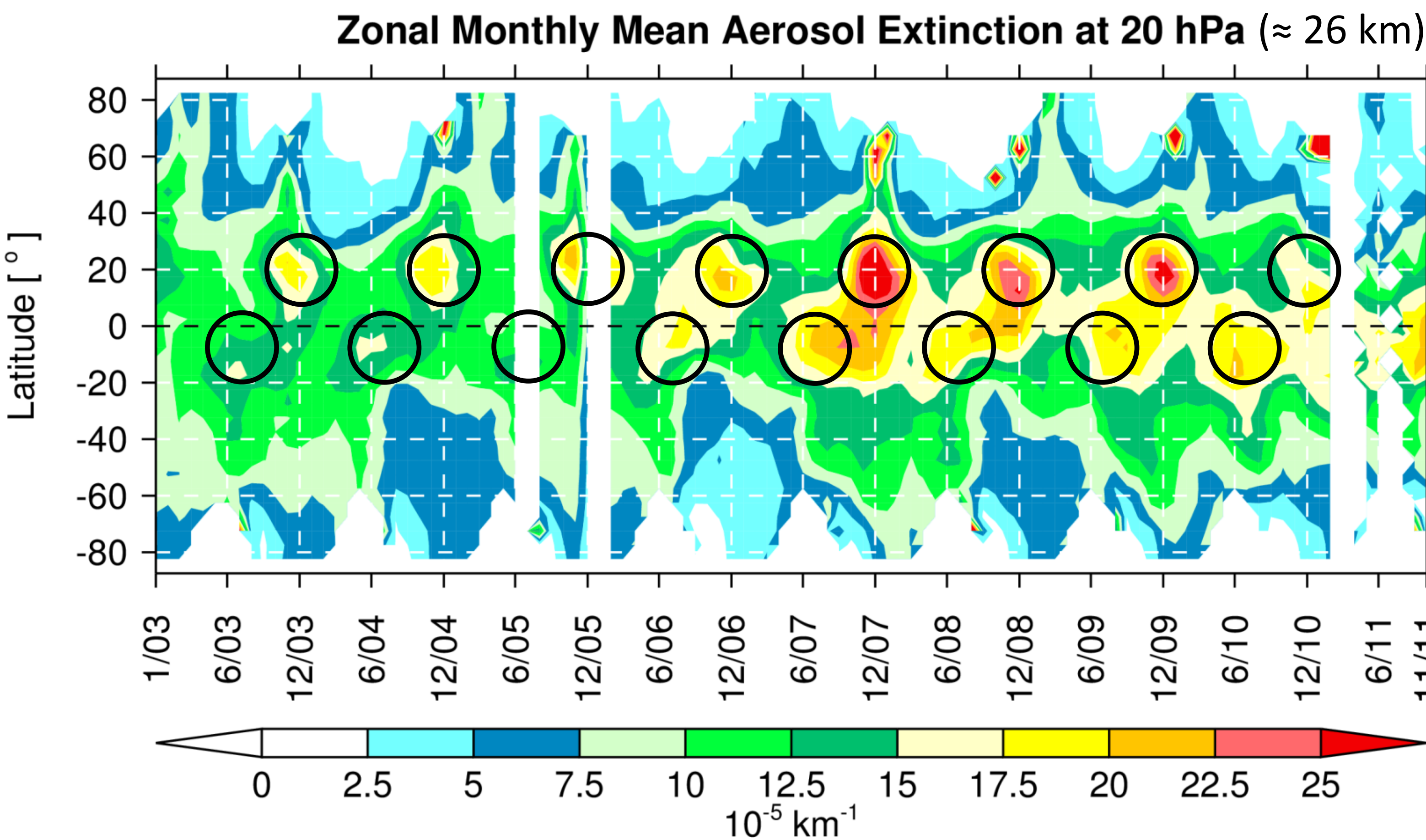

Universität Bremen*

Seasonal cycle

… can be explained by the Brewer-Dobson circulation, which is

1. stronger in the winter hemisphere **2. stronger in the northern hemisphere**

Zonal Monthly Mean Aerosol Extinction at 20 hPa (≈ 26 km)

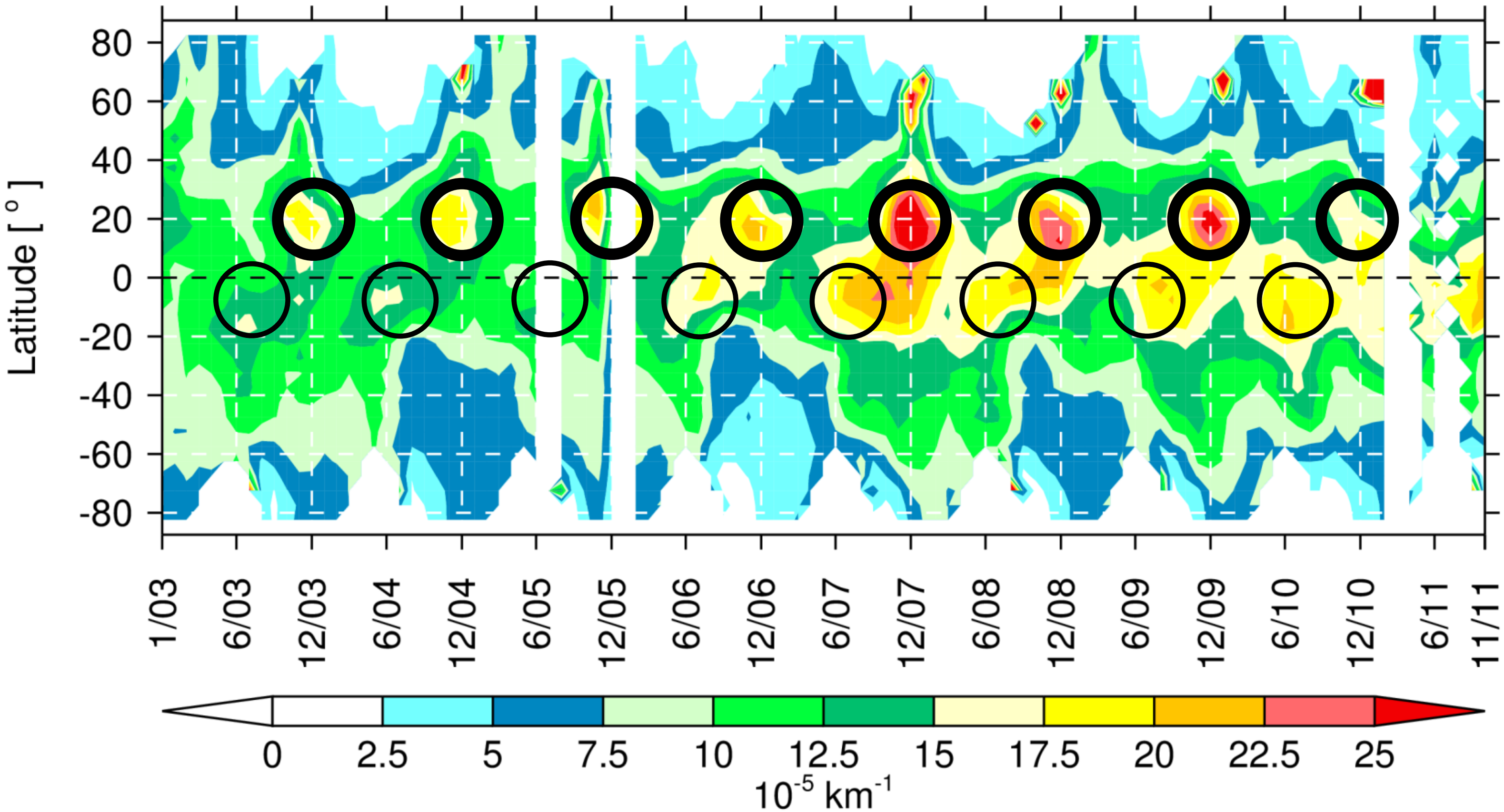

Latitude-time cross section at **10 hPa** (≈ 32 km)

Biennial variation

enhanced aerosol load about every 2 years.

Zonal Monthly Mean Aerosol Extinction at 10 hPa (≈ 32 km)

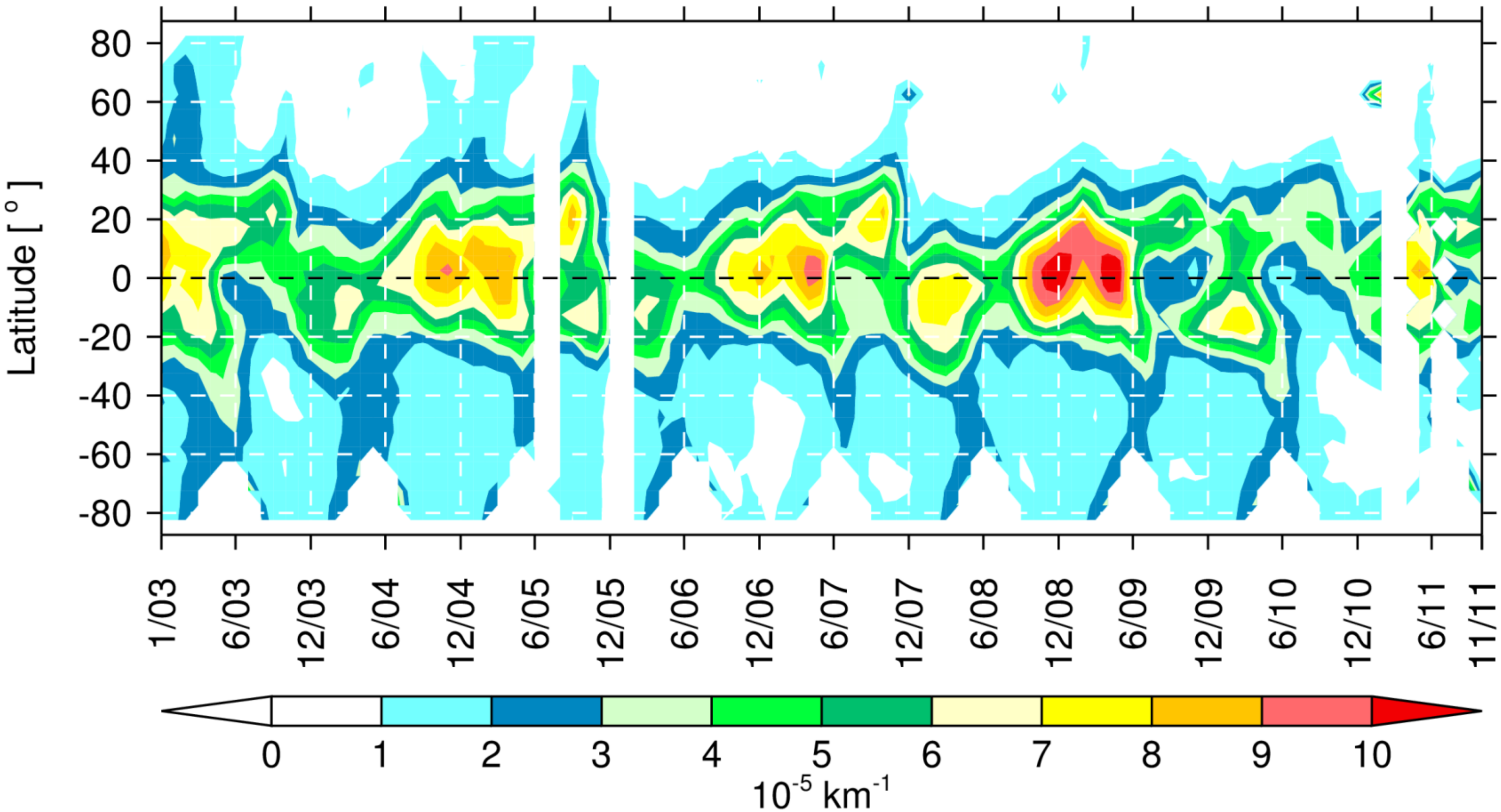

Biennial variation

… is indirectly due to the Quasi Biennial Oscillation (QBO).

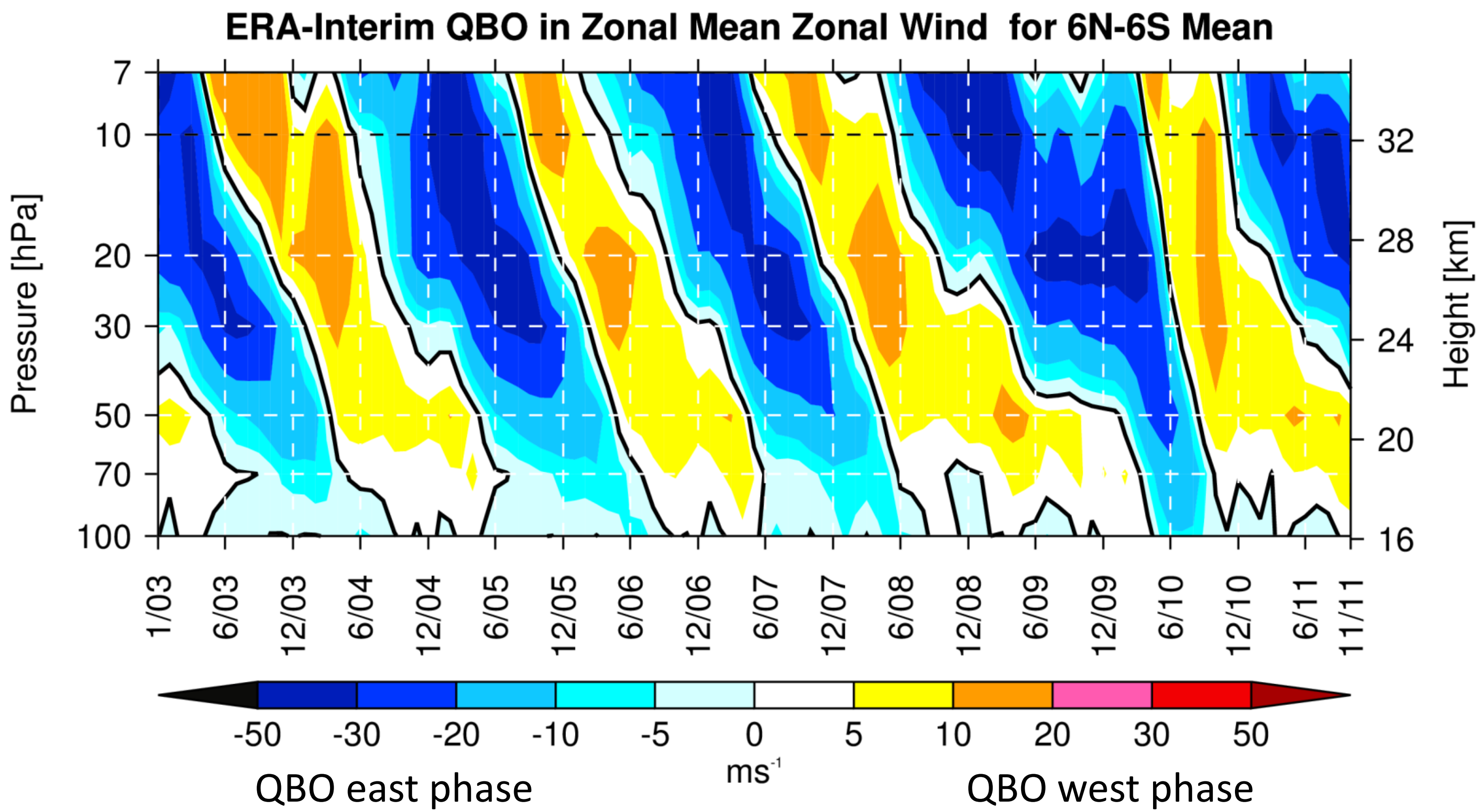

Biennial variation

ES = QBO **E**asterly **S**hear

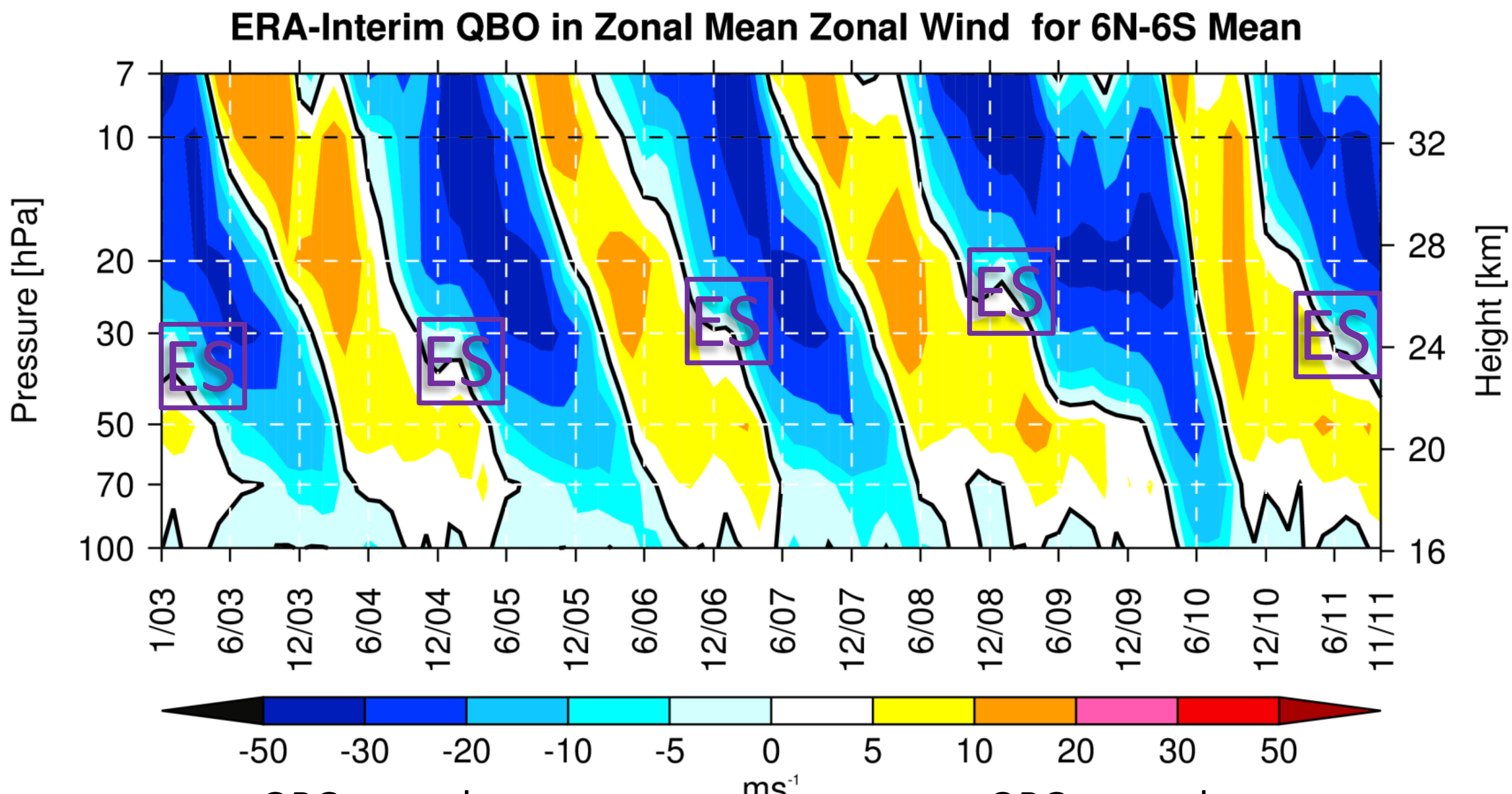

Universität Bremen*

Biennial variation

… is directly due to the "**secondary circulation of the QBO**"

ES = QBO **E**asterly **S**hear → meridional convergence

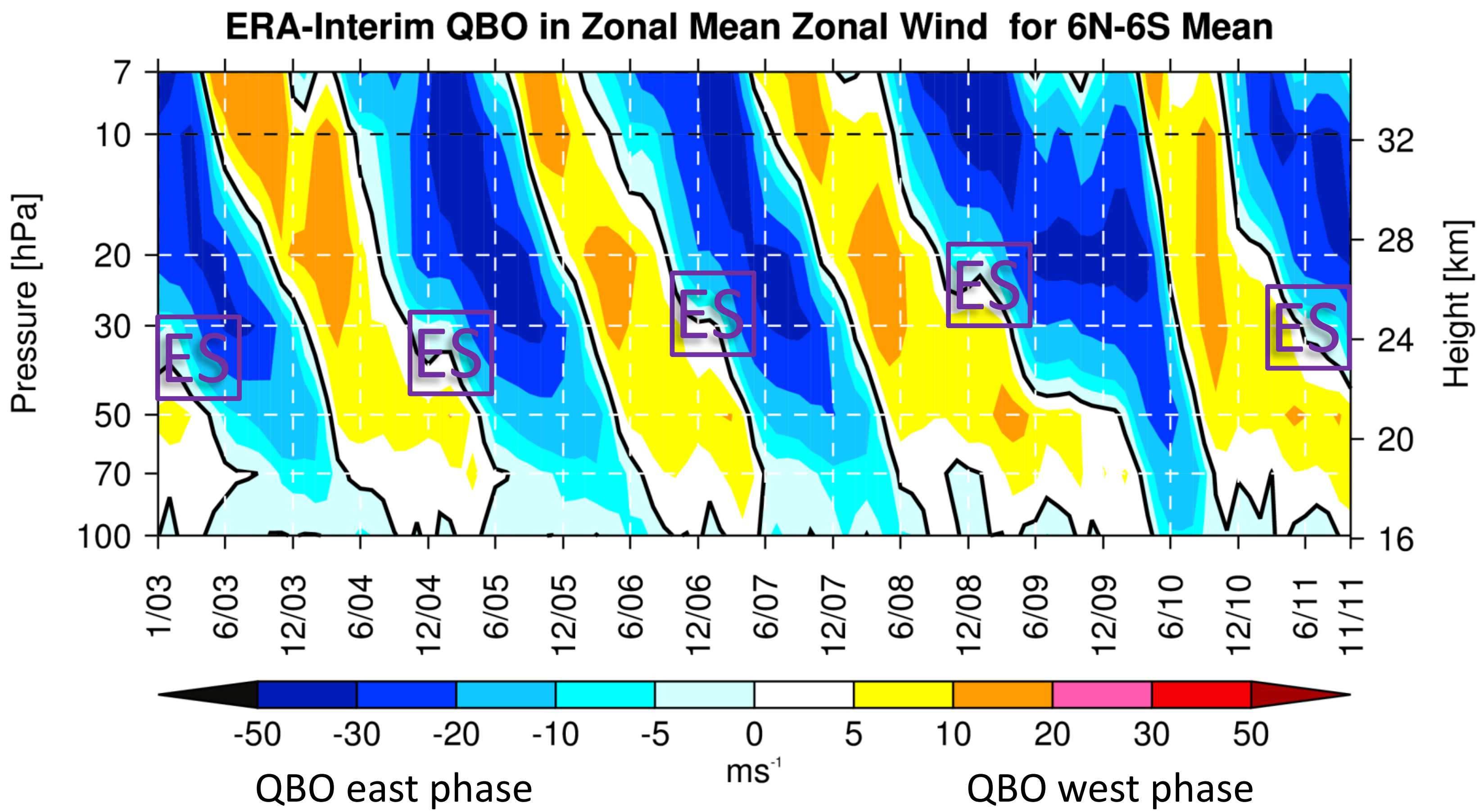

Biennial variation

… is directly due to the "**secondary circulation of the QBO**"

ES = QBO **E**asterly **S**hear → meridional convergence → more aerosols at higher altitudes

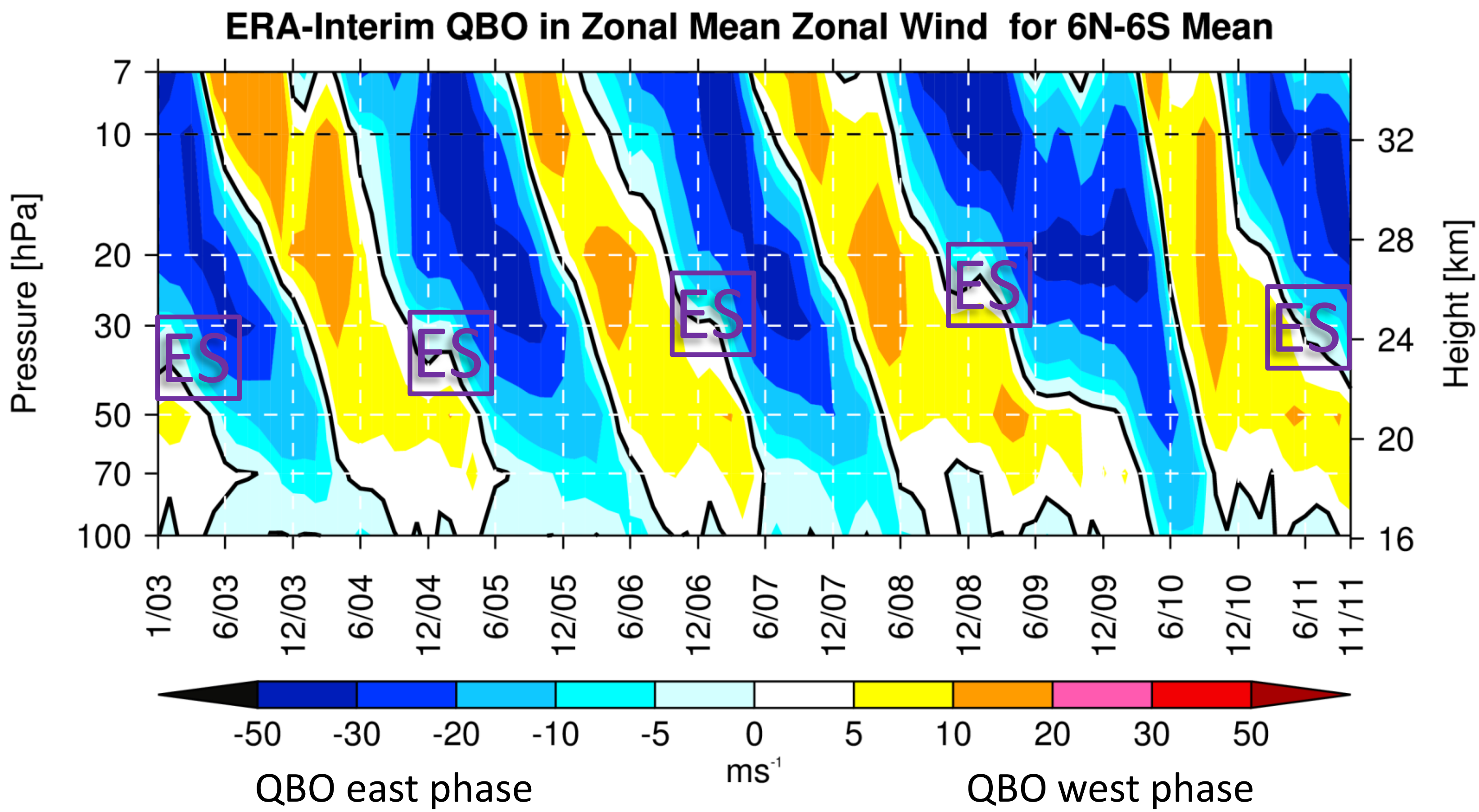

Biennial variation

… is directly due to the "**secondary circulation of the QBO**"

ES = QBO **E**asterly **S**hear → meridional convergence → more aerosols at higher altitudes

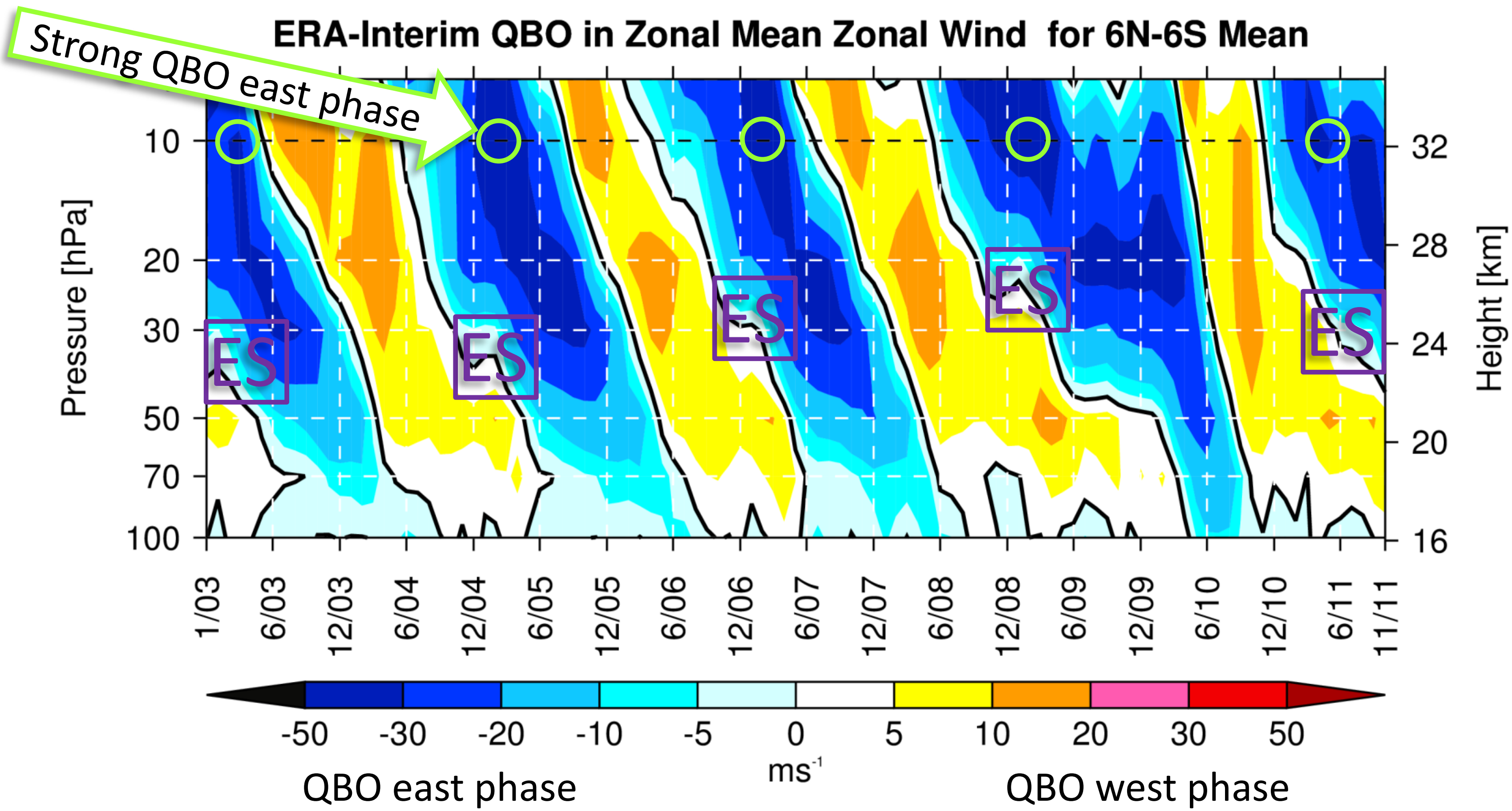

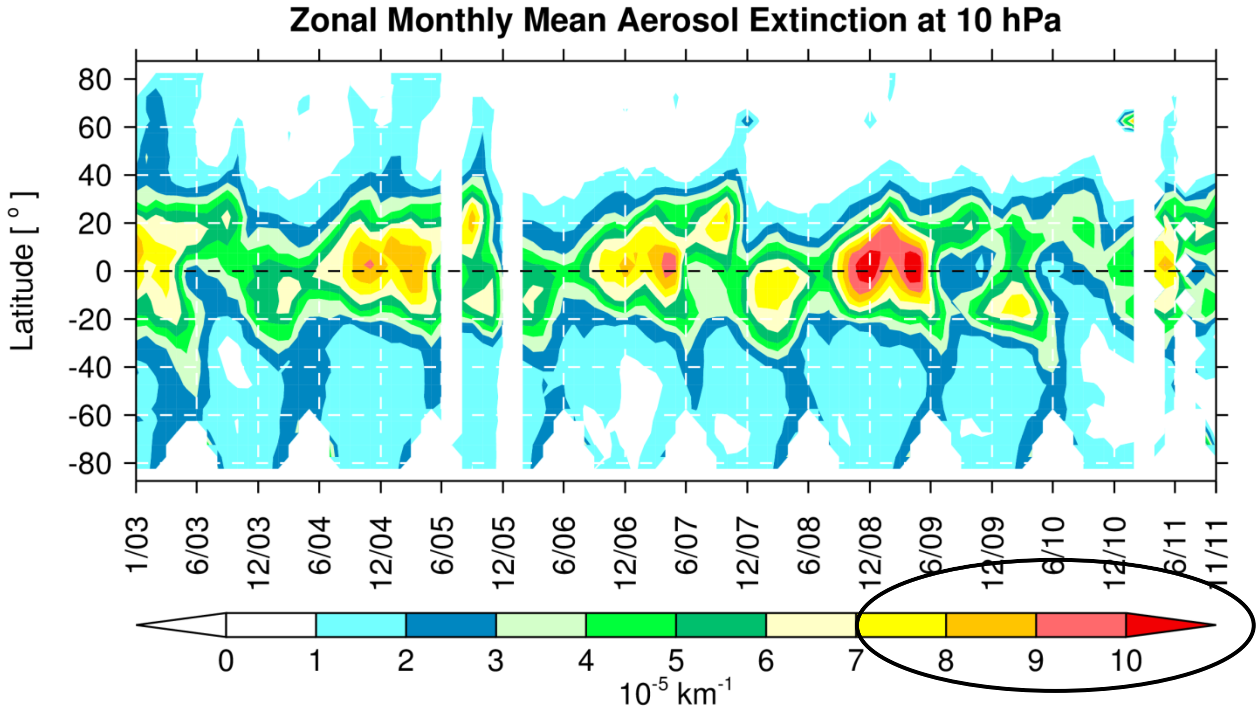
Zonal Monthly Mean Aerosol Extinction at 10 hPa
Latitude [°]
80 60 40 20 0 -20 -40 -60 -80
1/03 6/03 12/03 6/04 12/04 6/05 12/05 6/06 12/06 6/07 12/07 6/08 12/08 6/09 12/09 6/10 12/10 6/11 11/11
0 1 2 3 4 5 6 7 8 9 10
10^-5 km^-1

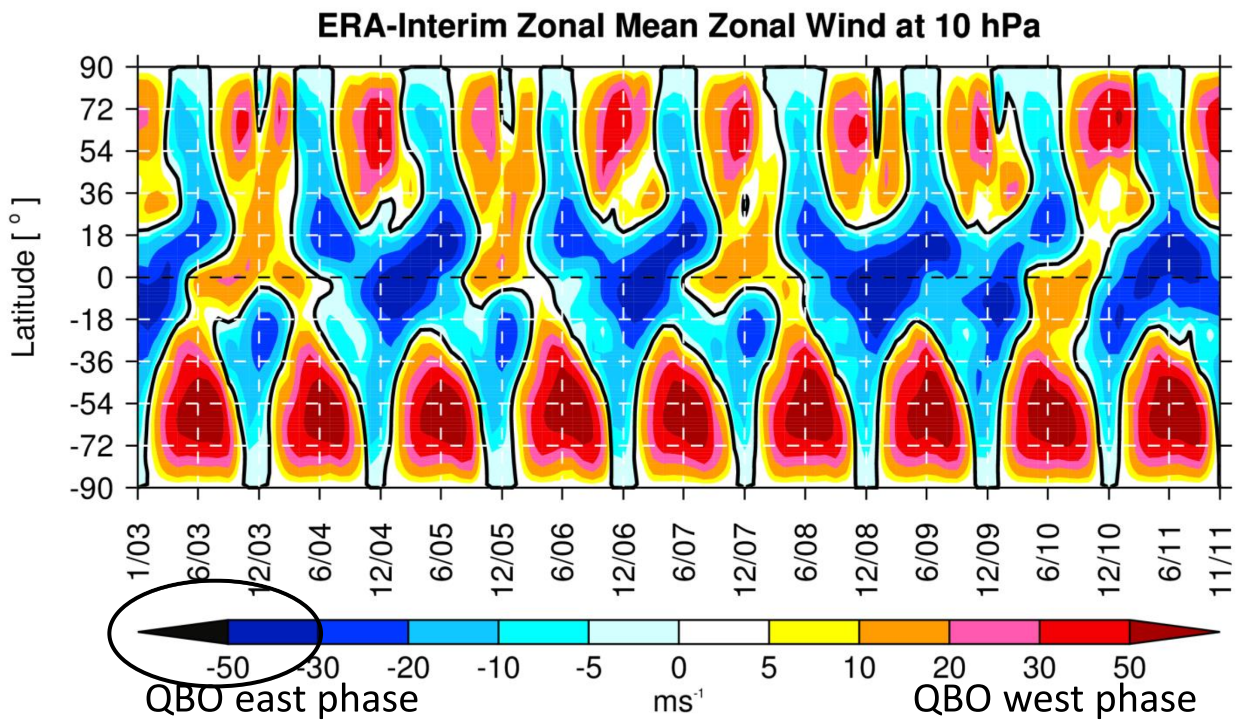
ERA-Interim Zonal Mean Zonal Wind at 10 hPa
Latitude [°]
90 72 54 36 18 0 -18 -36 -54 -72 -90
1/03 6/03 12/03 6/04 12/04 6/05 12/05 6/06 12/06 6/07 12/07 6/08 12/08 6/09 12/09 6/10 12/10 6/11 11/11
-50 -30 -20 -10 -5 0 5 10 20 30 50
ms^-1
QBO east phase
QBO west phase

Biennial variation

… correlates with a strong QBO east phase.

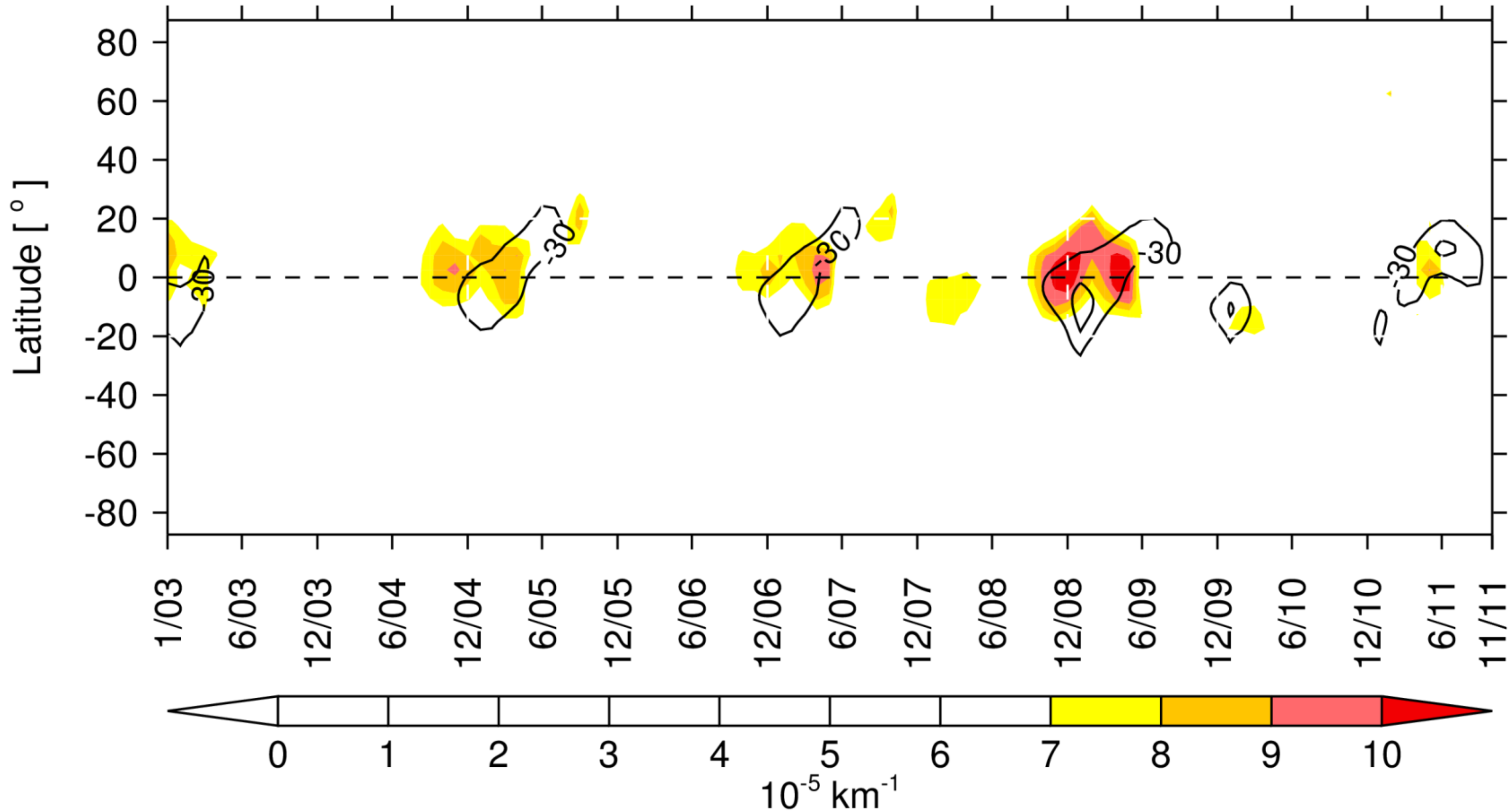

Black contour lines correspond to wind velocities < -30 m/s.

Outline

1. Climatological interpretation of the SCIAMACHY stratospheric aerosol data set (V1.1)

2. Outlook
   I) trend analysis
   II) the estimation of the stratospheric aerosol particle size distribution

Increase in the stratospheric aerosol load

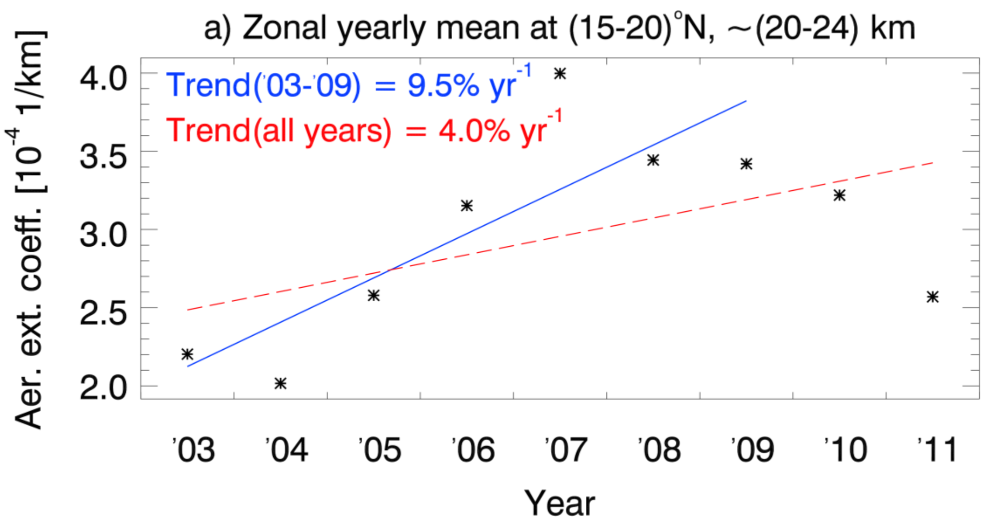

Hofmann et al., 2009:

Mauna Loa Observatory, Hawaii (~19°N) integrated lidar backscatter at 20-25 km from **2000-2009**:

Average trend = 4.8% yr^{-1}

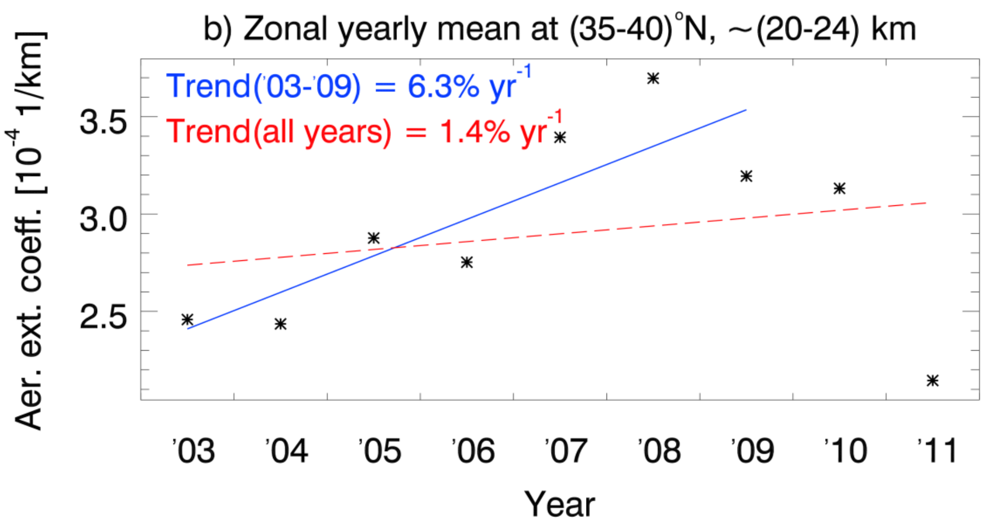

Boulder Observatory, Colorado (~40°N) integrated lidar backscatter at 20-25 km from **2001-2009**:

Average trend = 6.3% yr^{-1}

Increase in the stratospheric aerosol load

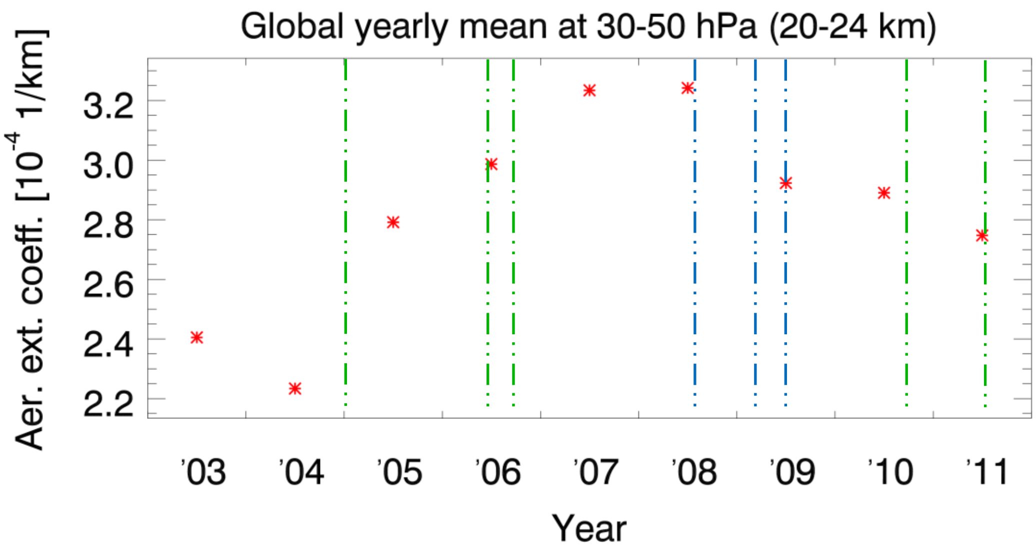

- For pressure levels > 10 hPa, increase in the aerosol load at all levels betw. 70-20 hPa
- The higher the pressure level, the stronger is the increase
- For pressure levels ≤ 10 hPa (≈ 32 km), slight decrease

–·–·– tropical volcanic eruption/bushfire
–·–·– non-tropical volcanic eruption/bushfire

Outlook: Linear regression analysis

Outline

1. Climatological interpretation of the SCIAMACHY stratospheric aerosol data set (V1.1)

2. Outlook
   I) trend analysis
   II) the estimation of the stratospheric aerosol particle size distribution

Change of the phase function with median radius

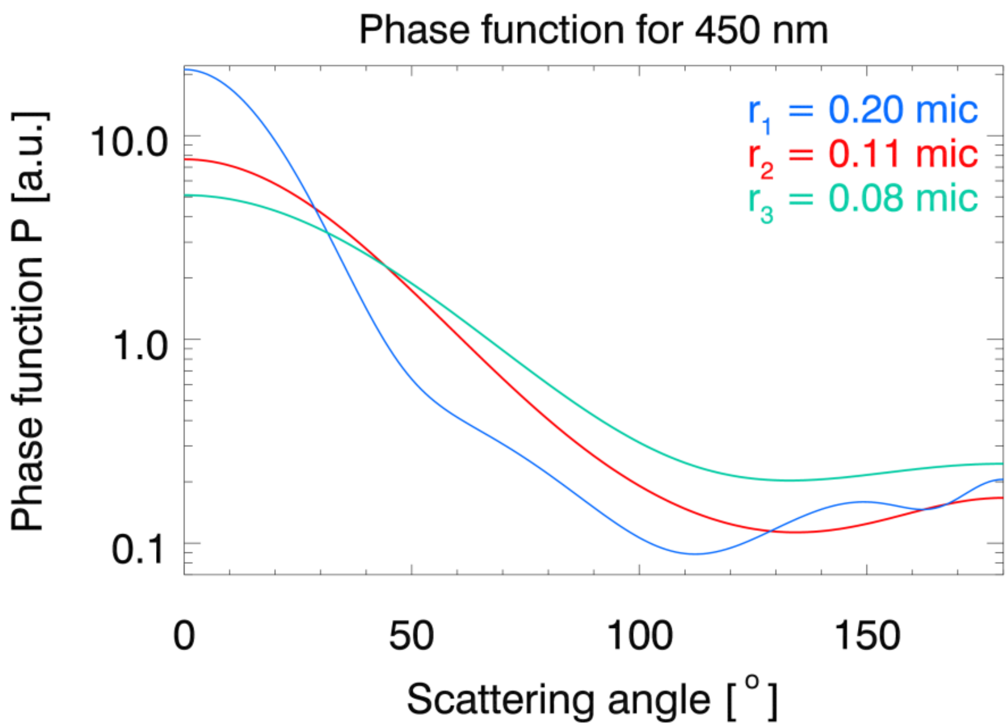

The relative difference between these phase functions is up to 180%.

Using a monomodal lognormal particle size distribution with σ = 1.37 like Deshler (2008).

Change of the phase function with median radius

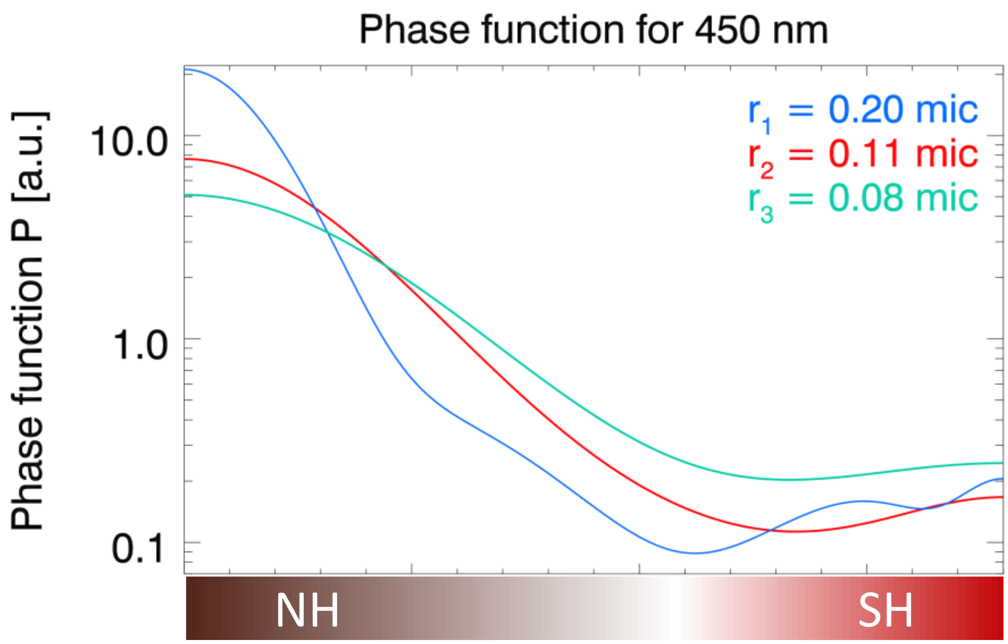

Related to the SCIAMACHY measurement geometry

The relative difference between these phase functions is up to 180%.

Estimate of the particle size distribution

Generating the measurement vector

1. $\boldsymbol{I}_N^{\lambda}(TH) = \boldsymbol{I}^{\lambda}(TH)/\boldsymbol{I}^{\lambda}(TH_{ref})$

   with $TH_{ref} = 35\,\mathrm{km}$

2. $\boldsymbol{y}(TH) = \ln\left(\frac{\boldsymbol{I}_N^{\lambda_l}(TH)}{\boldsymbol{I}_N^{\lambda_s}(TH)}\right)$

   with $\lambda_\mathrm{s} = 470\,\mathrm{nm}$ and $\lambda_\mathrm{l} = 750\,\mathrm{nm}$

Estimate of the particle size distribution

Generating the measurement vector

1. $\boldsymbol{I}_N^{\lambda}(TH) = \boldsymbol{I}^{\lambda}(TH)/\boldsymbol{I}^{\lambda}(TH_{ref})$

with $TH_{ref} = 35\,\mathrm{km}$

2. $\boldsymbol{y}(TH) = \ln\left(\frac{\boldsymbol{I}_N^{\lambda_l}(TH)}{\boldsymbol{I}_N^{\lambda_s}(TH)}\right)$

with $\lambda_s = 470\,\mathrm{nm}$ and $\lambda_l = 750\,\mathrm{nm}$

Several single wavelengths λ_i

$$\boldsymbol{y}(TH) = \ln\left(\boldsymbol{I}_N^{\lambda_i}(TH)\right)$$

λ_i = (380, 470, 750, 1090, 1550) nm

Dependence of extinction on λ

Particle size distribution

Phase function, **extinction**

Summary

- The present IUP stratospheric aerosol data set (V1.1) clearly shows volcanic eruption and bushfire events.
- As stratospheric aerosols have lifetimes of several years, they are a good tracer for dynamic processes: In the data set …
  - … a seasonal cycle (at about 26 km) has been observed, which is caused by the Brewer-Dobson circulation.
  - … a biennial variation (at about 32 km) has been identified, which is due to the secondary circulation of the QBO.
- First results indicate a global increase in the stratospheric aerosol load at 18-26 km A linear regression analysis is planed here.
- Future work will focus on the estimation of the particle size distributions.

Selected references

A. E. **Bourassa**, D. A. Degenstein, R. L. Gattinger, and E. J. Llewellyn. Stratospheric aerosol retrieval with optical spectograph and infrared imaging system limb scatter measurements. J. Geophys. Res., 112(D10217), 2007.

T. **Deshler**. A review of global stratospheric aerosol: Measurement, importance, life cycle, and local stratospheric aerosol, Atmos. Res., 90, 223–232, doi:10.1016/j.atmosres.2008.03.016, 2008.

D. **Hofmann**, J. Barnes, M. O'Neil, M. Trudeau, and R. Neely. Increase in background stratospheric aerosol observed with lidar at mauna loa observatory and Boulder, Colorado. Geophys. Res. Lett., 36:L15808, 2009.

J. L. **Neu**, L. C. Sparling, and R. A. Plumb. Variability of the subtropical "edges" in the stratosphere. 108(D15), 4482, doi:10.1029/2002JD002706. J. Geophys. Res., 2003.

M. **Niwano**. S. Hayashida, H. Akiyoshi, and M. Takahashi. Seasonal cycle of Stratospheric Aerosol and Gas Experiment II near-background aerosol in the lower stratosphere. 114, D14306, doi:10.1029/2008JD009842. J. Geophys. Res., 2009.

C. D. **Rodgers**. Inverse Methods for Atmospheric Sounding: Theory and Practice. World Scientific, Singapore, 2000.

A. **Rozanov**, V. V. Rozanov, M. Buchwitz, A. Kokhanovsky, and J. P. Burrows. Sciatran 2.0 – a new radiative transfer model for geophysical applications in the 175-2400nm spectral region. Adv. Space Res., 36(5):1015–1019, 2005. doi: 10.1016/j.asr.2005.03.012.

V. V. **Rozanov**, M. Buchwitz, K.-U. Eichmann, R. de Beek, and J. P. Burrows. Sciatran - a new radiative transfer model for geophysical applications in the 240–2400nm spectral region: The pseudo-spherical version. Adv. Space Res., 29(11):1831–1835, 2002.

C. R. **Trepte** and M. H. **Hitchman**. Tropical stratospheric circulation deduced from satellite aerosol data. Nature 355, 626−628 (1992).